

Data Repository Item

METHODS AND SAMPLING

Palynology

Samples for palynological analysis were collected from the sedimentary beds underlying, intercalated with, and overlying the four basaltic units. Three sites of the central High Atlas (Oued Ammazine, Oued Lahr, and Tiourjdal) and two sites of the Argana basin (Alemnzi and Agouersouine; Fig. DR1) were investigated. Sediments at the base of the lower basalts and interlayered between the basaltic units are mainly siltstones. Relatively thin layers (less than 5 m) of limestones or dolomites can be traced for distances of 50 km from the northern Central High Atlas between the intermediate and upper and between the upper and recurrent basalts. Within the southern Central High Atlas sections (e.g. Tiourjdal) limestone beds occur only locally.

The palynological preparations were made both at the Section des Sciences de la Terre, University of Genève, Switzerland, and at the Sedimentary Organic Matter Laboratory of the Dipartimento di Scienze della Terra, University of Perugia, Italy, using a combination of several standard palynological preparation procedures (Faegri & Iversen, 1975; Doher, 1980; Heusser & Stock, 1984; Traverse 1988; Wood et al., 1996.). Palynological content was analyzed by transmitted light microscopy at Perugia University.

A semi-quantitative investigation was carried out for each slide to estimate the relative proportions of the organic constituents. A selection of observed sporomorphs is shown in Fig. DR2. All investigated black basal siltstones from the central High Atlas were rich in sporomorphs, and show an almost constant pollen assemblage. Argana samples show a high degree of darkness and oxidation and thus a relatively moderate number of palynomorphs were recognized. Semi-quantitative analyses of basal sedimentary layers collected close to the contact to the oldest basalts and of the only sporomorph-bearing interlayered sedimentary bed are listed in Table DR1. Author citations for the recorded species and the sampling location and stratigraphic position are listed in Table DR2 and Table DR3, respectively.

$^{40}\text{Ar}/^{39}\text{Ar}$ analyses

Detailed $^{40}\text{Ar}/^{39}\text{Ar}$ analytical results and ages were obtained on basalts from central High Atlas and Oujda basins. $^{40}\text{Ar}/^{39}\text{Ar}$ ages were determined by the incremental heating technique (laser or furnace) on plagioclase separates at the Geochronology Laboratory of the CNRS-UMR Geosciences AZUR Nice, France (samples AN16, AN37, AN133, AN174, AN160) and at the Berkeley Geochronology Center (BGC), Berkeley, USA (sample MOR14; Table DR4). Transparent plagioclase grains (50–200 μm size) were handpicked under a binocular microscope and then repeatedly cleaned ultrasonically in distilled water and, with the exception of MOR14, leached with hot HNO_3 for a few minutes in order to eliminate any remaining influence of surface alteration. Samples were irradiated in the nuclear reactor at McMaster University (Hamilton, Canada) in position 5C, and at the Oregon State University TRIGA (MOR14). The neutron fluence monitors used in the Nice (Hb3gr hornblende, 1072 Ma) and BGC (Fish Canyon sanidine, 28.02 Ma) experiments have been intercalibrated (Renne, 2000)..

Plagioclase separates analyzed in Nice were either step-heated with a high-frequency furnace system (sample AN16, AN37) or gas extraction was carried out with a 50W SYNRAD CO_2 continuous laser (AN133, AN160, AN174), purified in a Pyrex line directly connected to a VG3600 mass spectrometer working with a Baur-Signer source and a Balzers SEV 217 electron multiplier. Plagioclase separates of sample MOR14 were degassed incrementally with a CO_2 laser and analyzed using a MAP 215C mass spectrometer using facilities and methods described previously (Knight et al.,

2003). In Table DR4, all analytical data are corrected for backgrounds, radioactive decay, mass discrimination (monitored by regular analysis of air pipette volumes). Ages were calculated from these data after correction for K, Ca and Cl reactor-induced interferences. Correction factors for interfering neutron reactions (McMaster irradiation) are $(^{39}\text{Ar}/^{37}\text{Ar})_{\text{Ca}} = 7.3 \times 10^{-4} \pm 4\%$, $(^{36}\text{Ar}/^{37}\text{Ar})_{\text{Ca}} = 2.82 \times 10^{-4} \pm 1\%$, $(^{40}\text{Ar}/^{39}\text{Ar})_{\text{K}} = 2.97 \times 10^{-2} \pm 3\%$. Correction factors for interfering neutron reactions (OSU TRIGA irradiation) are $(^{39}\text{Ar}/^{37}\text{Ar})_{\text{Ca}} = 6.95 \times 10^{-4} \pm 1.3\%$, $(^{36}\text{Ar}/^{37}\text{Ar})_{\text{Ca}} = 2.65 \times 10^{-4} \pm 0.9\%$, $(^{40}\text{Ar}/^{39}\text{Ar})_{\text{K}} = 7.30 \times 10^{-4} \pm 12.6\%$. Steiger and Jäger (1977) decay constants are used.

The analytical error for the plateau age (79.9–99.6% of the total ^{39}Ar) is at the 2σ level and including error in the value of the J irradiation parameter. The larger uncertainties of plateau ages for sample AN16, AN160, and MOR14 are due, in part, to higher Ca/K inducing a high Ca interference correction, and related lower concentrations of radiogenic ^{40}Ar gas. Variations of $^{37}\text{Ar}_{\text{Ca}}/^{39}\text{Ar}_{\text{K}}$ observed in samples (Table DR4) are not strongly correlated with variations of the Ar-Ar ages and are likely related to primary chemical zoning within plagioclase.

Geochemistry of the basalts

Basaltic samples were collected in stratigraphic order from eight sections of the central High Atlas, five of the Argana basin and two of the Oujda basin. In the central High Atlas sections, basalts belonging to the lower to recurrent units are preserved and those analyzed are optically and compositionally fresh (Table DR5). In the Argana and Oujda basin the preserved basalts are geochemically similar, from bottom to top of the sampled sections to the central High Atlas lower and intermediate basalts. Substantial alteration affects most younger Argana and Oujda basalts ($\text{LOI} > 1.5 \text{ wt\%}$).

Major element (wt%) and Cr and Ni (ppm) whole-rock concentrations of little altered (e.g., $\text{LOI} < 1.8 \text{ wt\%}$, generally $< 1.0 \text{ wt\%}$) 72 basalts were measured by means of a Philips PW 2400 XRF at the University of Lausanne, Switzerland, adopting standard procedures, whereas trace element concentrations were analyzed at the University of Grenoble, France, by inductively coupled plasma-mass spectrometry (ICP-MS; Barrat et al., 1996). Detection limit and uncertainties for REE analyses are 0.05–1 ppm and less than 5%, respectively. Analyses of representative central High Atlas, Argana and Oujda basalts are listed in Table DR5.

Magnetostratigraphy of the basalts

Paleomagnetic analyses were carried out on about 175 cores from the 260 m thick continuous volcanic pile at Tiourjdal, central High Atlas. Between three and nine oriented drill cores were sampled from each of the 33 identified lava flows and from one 2 m thick interlayered sedimentary bed. The site mean results are summarized as tilt-corrected virtual geomagnetic poles (VGP's) in Table DR6. Measurements were performed using alternating field demagnetization techniques at the Berkeley Geochronology Center.

Figure DR3 shows thermal susceptibility data as well as alternating field demagnetization data of representative samples including the interlayered limestone bed. The susceptibility data in particular show unambiguously that the magnetic carrier in the sediments is titanomagnetite with a high unblocking temperature.

References of Data Repository item:

Barrat, J.A., Keller, F., Amosse, J., Taylor, R.N., Nesbitt, R.W., Hirata, T., 1996, Determination of rare earth elements in sixteen silicate references by ICP-MS after Tm addition and ion exchange separation: Geostandard Newsletters, v. 20, p. 133-.

- Boynton, W.V., 1984, Cosmochemistry of Rare Earth Elements: meteorite studies, in Henderson, P., ed., Rare Earth Element Geochemistry, Amsterdam, Elsevier, p. 63-114.
- Doher, L. I., 1980, Palynomorph preparation procedures currently used in the paleontology and stratigraphy laboratories. D.S. Geological Survey Circular, v. 830, p. 1-29.
- Faegri, K. and Iversen, J., 1975, *Textbook of pollen analysis*, New York, Hafner Press, pp. 295.
- Heusser, L. E. and Stock, C.E., 1984, Preparation techniques for concentrating pollen from marine sediments and other sediments with low pollen density: *Palynology*, v. 8, p. 225-227.
- Kirchvink, J.L., 1980, The least-squares line and plane and the analysis of paleomagnetic data: *Geophysical Journal of the Royal Astronomical Society*, v. 62, p. 699-718.
- Knight, K.B., Renne, P.R., Halkett, A., and White, N., 2003, $^{40}\text{Ar}/^{39}\text{Ar}$ dating of the Rajahmundry Traps, eastern India, and their relationship to the Deccan Traps: *Earth and Planetary Science Letters*, v. 208, p. 85-99.
- Onstott, T. C., 1980, Application of the Bingham distribution function in paleomagnetic studies: *Journal of Geophysical Research*, vol. 85, p. 1500-1510.
- Renne, P.R., 2000, $^{40}\text{Ar}/^{39}\text{Ar}$ age of plagioclase from Acapulco meteorite and the problem of systematic errors in cosmochronology: *Earth and Planetary Science Letters*, v. 175, p. 13-26.
- Renne, P.R., Swisher, C.C., Deino, A.L., Karner, D.B., Owens, T., and DePaolo, D.J., 1998, Intercalibration of standards, absolute ages and uncertainties in $^{40}\text{Ar}/^{39}\text{Ar}$ dating: *Chemical Geology (Isotope Geoscience Section)*, v. 145, p. 117-152.
- Steiger, R.H. and Jäger, E., 1977, Subcommission on geochronology: convention on the use of decay constants in geo and cosmochronology: *Earth Planetary Science Letters*, v. 36, p. 359-362.
- Traverse, A., 1988, Paleopalynology, Boston, London, Sydney, Wellington, Unwin Hyman, pp. 600.).
- Wood, G.D., Gabriel, A.M., and Lawson, J.C., 1996, in Jansonius, J. and McGregor, D.C., eds., *Palynology: principles and applications*, Toronto, Canada, American Association of Stratigraphic Palynologists Foundation, pp. 29-50.
- Zijderveld, J.D.A., 1967, A.C. demagnetisation of rocks: Analysis of results, in: *Methods in Palaeomagnetism*, pp. 254-286.

Data Repository item, Figure and Table captions

Figure DR1. Photograph of contact between basal gray mudstone AN131 and altered (reddish) lower basalt at Aguersouine, Argana.

Figure DR2. Microphotographs of most important sporomorphs of Moroccan samples listed in parentheses. Photographs 1-5: *Patinasporites densus* (1, 2: AN52b; 3: AN1; 4: AN69; 5: AN60); 6-10: *Corollina murphyae* (6: AN52b; 7, 10: AN50; 8, 9: AN69); 11, 12: *Classopollis torosus* (11: AN52b; 12: AN50); 13-15: *Gliscopollis meyeriana* (13, 15: AN50; 14 AN52); 16: *Calamospora mesozoica* (16: AN52b).

Figure DR3. Representative examples of demagnetization behavior, tilt corrected, plotted in stereographic projection and as orthogonal vector endpoint diagrams (Zijderveld, 1967). Lava directions were defined by principal component analysis (Kirchvink, 1980), and the reversed sediment direction was defined using great circle fits (Onstott, 1980). Examples are shown in relative stratigraphic order. Note the remagnetization of the top portion of the upper limits of the limestone horizon (27) by the overlying lava flow (28), yielding a positive baked contact test. Also shown are susceptibility vs. temperature curves for these horizons. The blue line shows relative susceptibility as a function of temperature, while the red line shows the averaged first derivative of susceptibility, highlighting the changes in slope. Curves for both the bracketing basalt flows as well as the sedimentary horizon show a distinct drop in susceptibility between 560 $^{\circ}$ - 580 $^{\circ}$ C, clearly indicating titanomagnetite as the main magnetic carrier for these samples. Curves do not show any significant shifts above this temperature precluding the presence of higher temperature magnetic carrier phases (e.g., hematite).

Table DR1. Semi-quantitative counting of sporomorphs of siltstones sampled at the base of the lower basaltic unit of the central high Atlas (CHA) and Argana basins and on top of the central High Atlas upper basalts (AN69). Categories are: Rare (R): 0-5 specimens; Common (C): 5-20 specimens; Frequent (F): 20-40 specimens; Abundant (A): more than 40 specimens. Sampling coordinates are listed in Table DR3.

Table DR2. Author citation for observed palynological species.

Table DR3. GPS coordinates of samples listed in Tables DR1, DR4, DR5.

Table DR4. $^{40}\text{Ar}/^{39}\text{Ar}$ analytical results obtained on plagioclase separates of central High Atlas and Oujda basalts analyzed at Nice and at the Berkeley Geochronology Center. $^{39}\text{Ar}(\%)$ = fraction of ^{39}Ar released for each step; $^{40}\text{Ar}_{\text{rad}}$ = radiogenic ^{40}Ar ; Ar_K et Ar_{Ca} = Ar produced respectively by K and Ca neutron interferences, according to $^{37}\text{Ar}_{\text{Ca}}/^{39}\text{Ar}_K$ ratio and atmospheric contamination level; J = irradiation parameter; a = steps not included in the plateau age calculation. All uncertainties, except on plateau age (2σ) are quoted at the 1σ level, and do not include the uncertainties on the age of the monitor (J). The uncertainties on the $^{40}\text{Ar}_{\text{rad}}/^{39}\text{Ar}_K$ ratio of the monitor are included in the calculation of the plateau age uncertainty.

Table DR5. Major (wt%) and trace element (ppm) compositions of representative central High Atlas (CHA), Argana and Oujda basalts of the lower, intermediate (inter), upper, and recurrent basalts. Chondrite normalized, cn (Boynton, 1984), La/Yb are reported. Sampling coordinates are listed in Table DR3.

Table DR6. Mean flow tilt corrected VGP latitude and longitude for the about 260m thick central High Atlas Tiourjdal section of Central Atlantic magmatic province volcanics and sediments ($N31^{\circ} 07' 74''$, $W7^{\circ} 22' 70''$). n = number of cores analyzed for each site. Tilt correction applied to the Tiourjdal flows is 12° - 15° dip, with 200° - 205° dip direction.

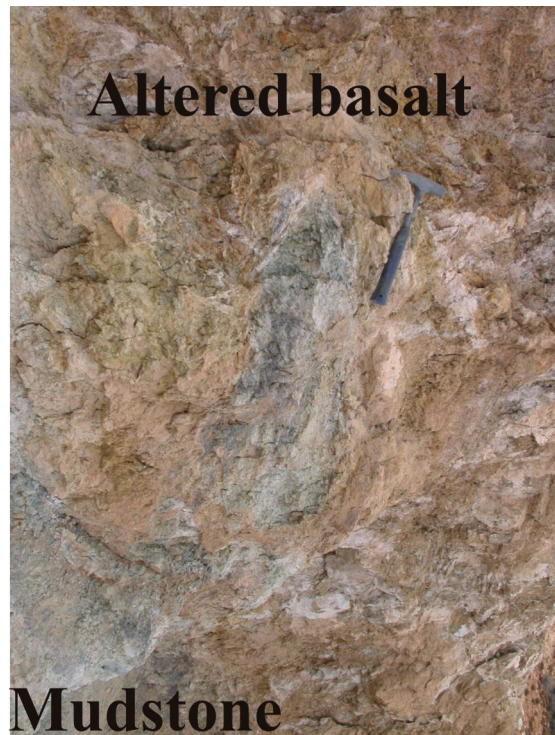


Figure DR1

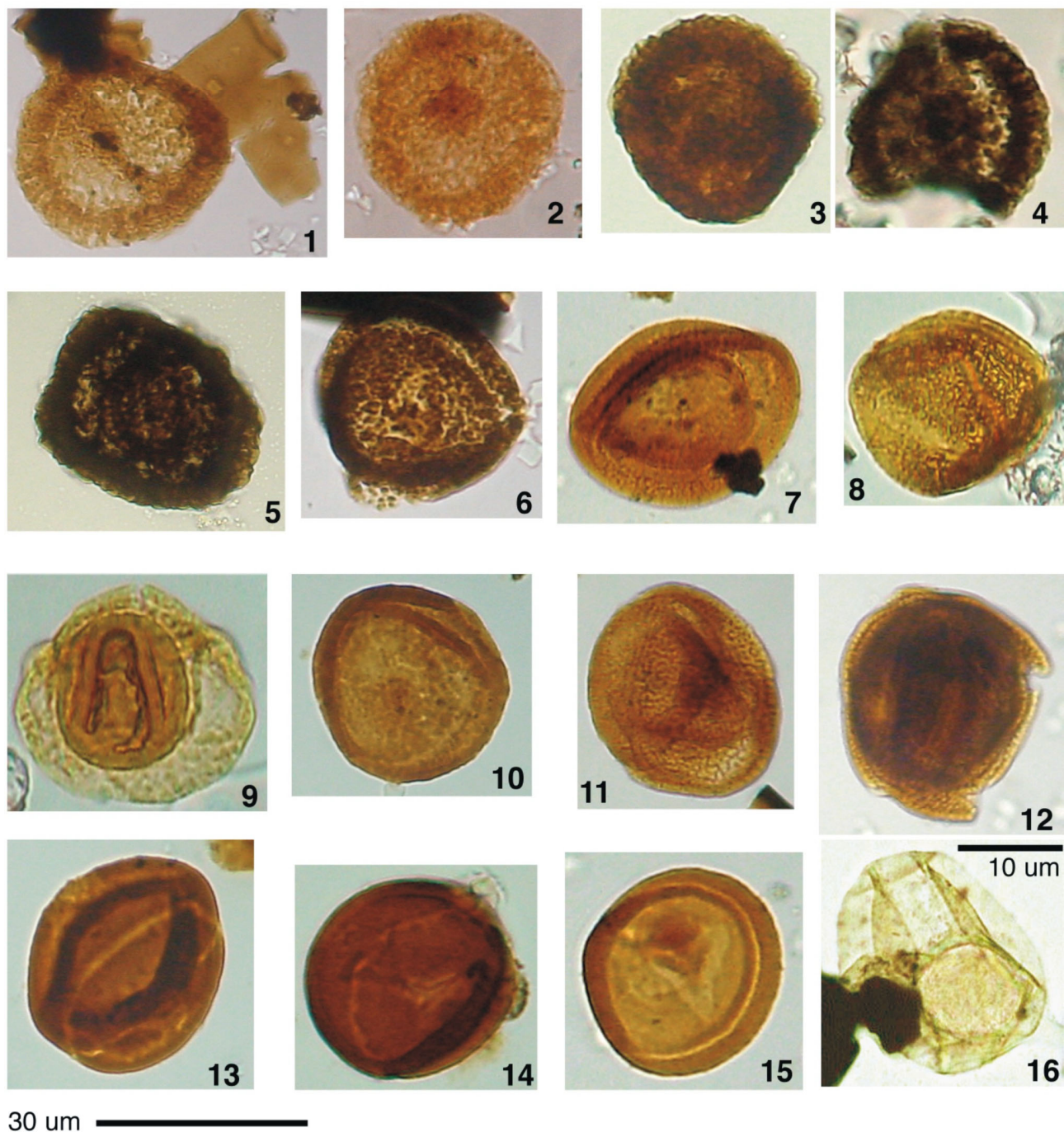


Figure DR2

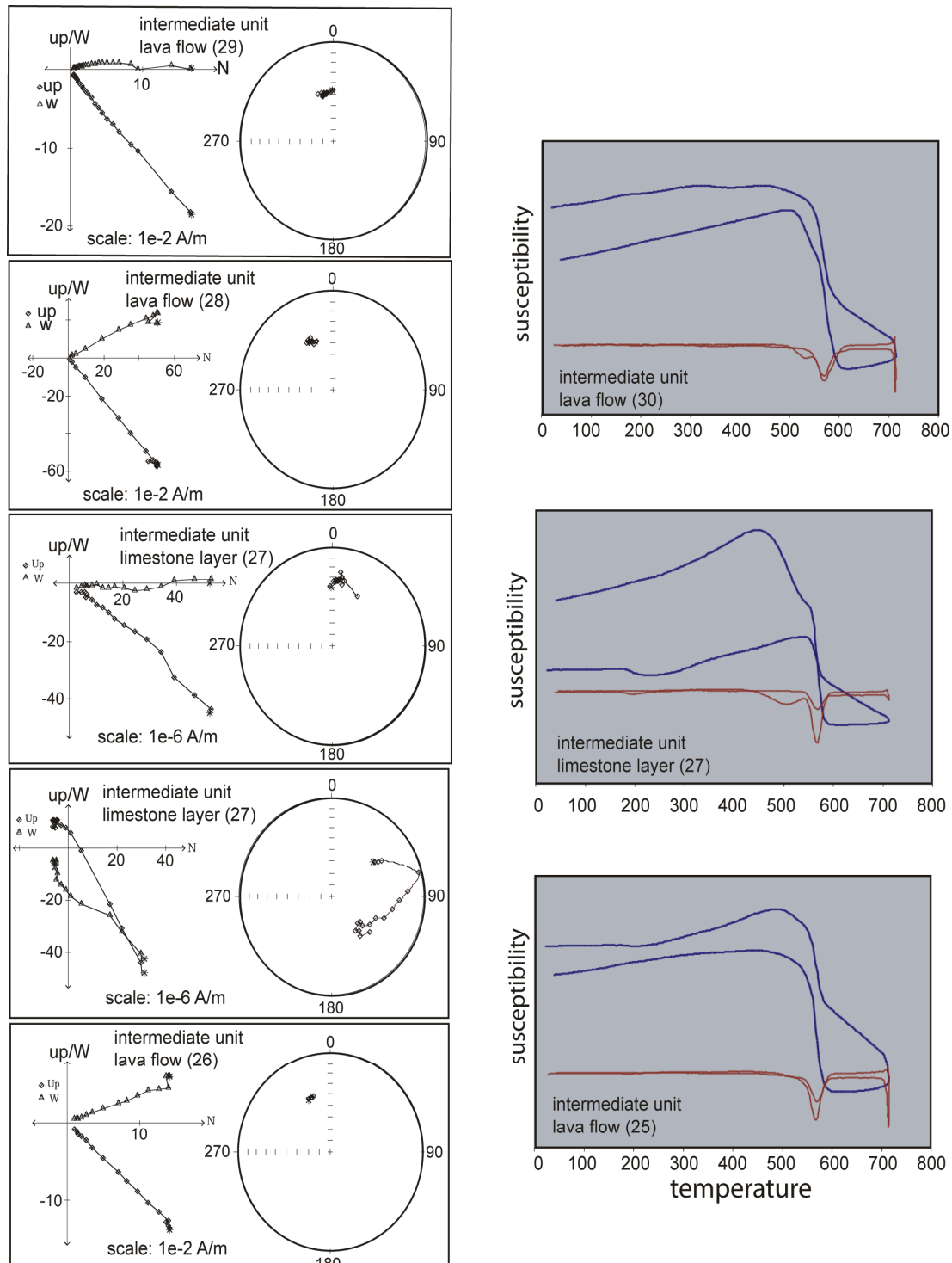
**Figure DR3**

Table DR1: semi quantitative counting of sporomorphs.

sample	AN50	AN52	AN52b	AN60	AN59	AN69	AN1	AN131	AN101
Stratigraphic position	50cm below lower basalt	15cm below lower basalt	<5cm below lower basalt	25cm below lower basalt	<5cm below lower basalt	50cm above upper basalt	35cm below lower basalt	<5 cm below lower basalt	20cm below lower basalt
section basin	Tiourjdal CHA			Oued Lahr CHA			Oued Amazine CHA	Alemzi Argana	Aguersouine Argana
<i>P. densus</i>	F	A	A	F	A	R	F	R	R
<i>G. meyeriana</i>	F	C	F	F	F		R	F	R
<i>C. murphyae</i>	A	F	C	C	C	A	R	C	R
<i>C. torosus</i>	C	C	C	R	C	C		R	
<i>D. velatus</i>	R								
<i>I. parvisaccatus</i>	R								
<i>P. papilionis</i>	R								
<i>E. troedssonii</i>	R								
<i>C. cameronii</i>	C								
<i>V. pallidus</i>	R	R							
<i>C. mesozoica</i>	C			R	R	R	R	R	
<i>Alisporites</i> sp.	R	R	C	R	R	R	R	R	
<i>Cycadopites</i> sp.	R								
<i>D. mortonii</i>		R							
<i>Triadispora</i> sp.			R		R			R	
<i>A. tenuicorpi</i>				R					
<i>P. triassicus</i>				R					
<i>E. chinleana</i>				R					
<i>A. australis</i>				R					
<i>S. foveorugulata</i>			R						
<i>A. tenuicorpus</i>			R						
<i>Tsugaepollenites</i> sp.				R				R	
<i>Schizosaccus</i> sp.				R	R				
<i>R. tuberculatus</i>				R					R
<i>Todisporites</i> sp.				R				R	R
undet. Bisaccate	R	R	C	C	C		C	R	R

Table DR2: author citation for observed palynological species.

- Alisporites australis*, de Jersey, 1962
Alisporites tenuicorpus, Balme, 1970
Araucariacites australis, Cookson, 1947
Calamospora mesozoica, Couper, 1958
Classopollis torosus, (Reissinger) Balme, 1957
Con verrucosporites cameronii, Playford and Dettmann, 1965
Corollina murphyae, Fowell and Traverse, 1995
Densoisporites velatus, Weyland and Krieger, 1953
Ephedra chinleana, (Daugherty) emend. Scott, 1960
Eucommiidites troedssonii, Erdtman, 1948
Dictyophyllidites mortonii, (de Jersey) Playford & Dettmann, 1965
Gliscopollis meyeriana, (Klaus, 1960) Venkatachala, 1966
Indusiisporites parvisaccatus, de Jersey, 1963
Lycopodiacidites rugulatus, (Couper, 1958) Schulz, 1967
Patinasporites densus, Leschik, 1956 emend. Scheuring, 1970
Perinopollenites elatoides, Couper, 1958
Platysaccus papilionis, Potonié et Klaus, 1954
Parvisaccites triassicus, Scheuring, 1978
Ricciisporites tuberculatus, Lundblad ,1954
Sellaspora foveorugulata, Van der Eem, 1983
Vitreisporites pallidus, (Reissinger, 1950) Nilsson, 1958

Table DR3: sampling localities and GPS coordinates.

sample	rock-type	stratigraphic position	area	latitude N	longitude W	basin	
AN24	basalt	recurrent	Ait Ourir	31° 32' 50"	7° 40' 20"	northern central High Atlas	
AN22	basalt	upper					
AN18	basalt	intermediate					
AN16	basalt	lower					
AN63	basalt	upper	Ikourker	31° 37' 58"	7° 30' 81"	northern central High Atlas	
AN32	basalt	Lower					
AN39	basalt	intermediate	Jebel Imizar	31° 35' 48"	7° 25' 46"		
AN37	basalt	lower					
AN69	limestone	top of upper basalt	Oued Lahr	31° 36' 45"	7° 22' 53"	northern central High Atlas	
MOR14	basalt	upper					
AN59	siltstone	base of lower basalts					
AN60	siltstone	base of lower basalts					
AN1	siltstone	base of lower basalts	Oued Amazine	31° 35' 03"	7° 22' 17"	northern central High Atlas	
AN169	basalt	recurrent	Telouet	31° 15' 83"	7 17' 29"		
AN164	basalt	upper					
AN160	basalt	intermediate					
AN156A	basalt	recurrent	Tazgaoute	31° 10' 44"	7° 29' 82"	northern central High Atlas	
AN44	basalt	recurrent	Agouim	31° 10' 25"	07° 27' 22"		
AN57	basalt	upper					
AN56	basalt	intermediate					
AN141	basalt	upper	Tiourjdal	31° 07' 74"	7° 22' 70"	southern central High Atlas	
AN138	basalt	intermediate					
AN137A	basalt	intermediate					
AN136	basalt	lower					
AN134	basalt	lower					
AN133	basalt	lower					
AN49	basalt	lower					
AN52b	siltstone	base of lower basalts					
AN52	siltstone	base of lower basalts	Alemzi	30° 43' 71"	9 14' 47"	Argana	
AN50	siltstone	base of lower basalts					
AN132	basalt	lower					
AN31	siltstone	base of Lower basalts	Agouersuine	30° 44'	9° 15'		
AN129	basalt	intermediate	Tasgouint	30° 43' 95"	9° 15' 45"	Argana	
AN130	basalt	lower					
AN101	siltstone	base of lower basalts	Alemzi	30° 43' 71"	9 14' 47"	Oujda	
AN174B	basalt	lower	Oujda	34° 18' 94"	2° 6' 94"		

Table DR4: $^{40}\text{Ar}/^{39}\text{Ar}$ geochronology of Moroccan CAMP basalts

non radiogenic ^{40}Ar (%)	^{39}Ar (%)	$^{37}\text{Ar}_{\text{Ca}}/^{39}\text{Ar}_{\text{K}}$ $\pm 1\sigma$	$^{40}\text{Ar}_{\text{rad}}/^{39}\text{Ar}_{\text{K}}$ $\pm 1\sigma$	Age (Ma) $\pm 1\sigma$
Central High Atlas (lower basalts / Aït Ourir) – Sample AN16 - analyzed at Nice (J = 0.01477; weight = 19 mg)				
Temperature (°C)				
550	98.4	0.1	3.30 ± 0.10	6.85 ± 5.72
650 ^a	91.5	0.8	9.90 ± 0.10	6.73 ± 0.95
700 ^a	75.3	1.5	18.80 ± 0.10	6.28 ± 0.33
50 ^a	61.1	5.7	25.64 ± 0.09	7.63 ± 0.19
800	34.9	8.9	27.56 ± 0.05	7.70 ± 0.09
850	34.6	12.8	27.58 ± 0.07	7.74 ± 0.09
900	36.2	12.1	27.62 ± 0.04	7.74 ± 0.09
950	49.1	9.8	27.26 ± 0.08	7.76 ± 0.13
1000	61.2	16.3	26.67 ± 0.06	8.36 ± 0.19
1100	67.6	10.8	25.10 ± 0.07	8.47 ± 0.26
1170	49.0	5.2	24.63 ± 0.09	7.87 ± 0.14
1250	68.1	2.7	25.30 ± 0.10	7.55 ± 0.27
1300	50.5	2.9	24.60 ± 0.09	7.63 ± 0.14
1350	56.6	1.4	26.20 ± 0.10	7.51 ± 0.25
1400	49.7	2.7	27.50 ± 0.10	7.85 ± 0.16
1450	64.4	5.2	30.86 ± 0.09	8.00 ± 0.22
1500	35.6	1.1	31.90 ± 0.30	7.70 ± 0.26
1600 – Fuse ^a	93.8	0.1	30.20 ± 0.90	2.16 ± 2.13
				Integrated age (2σ)
				198.8 ± 2.6
				Plateau age (2σ)
				200.3 ± 2.6
Central High Atlas (lower basalt / Jebel Imizar) – Sample AN37 - analyzed at Nice – (J^b = 0.01493 ; weight = 41 mg)				
Temperature (°C)				
550 ^a	96.2	0.02	10.9 ± 0.4	7.2 ± 4.1
650 ^a	72.7	0.4	11.30 ± 0.08	9.40 ± 0.50
700 ^a	27.0	1.0	13.06 ± 0.05	8.10 ± 0.08
750 ^a	10.7	2.1	15.18 ± 0.05	7.95 ± 0.06
800	4.3	8.0	19.32 ± 0.05	7.83 ± 0.04
850	2.4	14.1	19.80 ± 0.03	7.83 ± 0.04
900	2.0	15.2	17.37 ± 0.03	7.83 ± 0.04
950	2.0	12.8	16.78 ± 0.03	7.81 ± 0.03
1000	1.9	13.5	15.87 ± 0.03	7.84 ± 0.03
1050	1.8	7.2	14.57 ± 0.03	7.86 ± 0.03
1100	2.2	6.4	8.75 ± 0.03	7.82 ± 0.03
1150	3.1	3.3	10.17 ± 0.03	7.87 ± 0.04
1200	1.8	2.0	17.54 ± 0.06	7.89 ± 0.05
1250	3.5	1.8	21.59 ± 0.08	7.75 ± 0.05
1300	2.8	1.8	22.20 ± 0.09	7.77 ± 0.07
1350	1.6	1.1	23.49 ± 0.10	7.76 ± 0.09
1400	2.3	3.6	24.16 ± 0.06	7.78 ± 0.05
1450	3.2	5.5	29.68 ± 0.03	7.79 ± 0.05
1500 ^a	19.6	0.3	31.6 ± 0.6	8.14 ± 0.69
1600 – Fuse ^a	84.3	0.01	23.0 ± 1.0	19.7 ± 10.7
				Integrated age (2σ)
				199.7 ± 0.6
				Plateau age (2σ)
				199.3 ± 0.6

Table DR4, continuation: $^{40}\text{Ar}/^{39}\text{Ar}$ geochronology of Moroccan CAMP basalts

non radiogenic ^{40}Ar (%)	^{39}Ar (%)	$^{37}\text{Ar}_{\text{Ca}}/^{39}\text{Ar}_{\text{K}}$ $\pm 1\sigma$	$^{40}\text{Ar}_{\text{rad}}/^{39}\text{Ar}_{\text{K}}$ $\pm 1\sigma$	Age (Ma) $\pm 1\sigma$
Central High Atlas (lower basalts / Tiourjdal) – Sample AN133 – analyzed at Nice (J=0.01734 ; ~ 100 grains)				
Laser steps				
1 ^a	83.8	0.4	10.5 ± 0.1	7.09 ± 0.70
2	18.4	5.4	18.05 ± 0.06	6.75 ± 0.07
3	6.9	8.0	19.26 ± 0.04	6.72 ± 0.05
4	3.6	10.4	20.06 ± 0.03	6.74 ± 0.06
5	2.9	14.2	19.76 ± 0.03	6.69 ± 0.04
6	2.4	12.3	19.35 ± 0.03	6.69 ± 0.04
7	2.2	13.2	19.37 ± 0.06	6.68 ± 0.05
8	2.0	11.0	19.86 ± 0.10	6.71 ± 0.06
9	1.6	10.6	19.18 ± 0.10	6.75 ± 0.07
10 - Fuse	1.8	14.5	21.40 ± 0.04	6.74 ± 0.05
Integrated age (2 σ)				198.7 ± 1.0
Plateau age (2 σ)				198.7 ± 1.0
OUJDA (lower basalt / Oujda) – Sample AN174 – analyzed at Nice (J =0.01737 ; ~ 100 grains)				
Laser steps				
1 ^a	74.0	0.6	2.36 ± 0.04	7.39 ± 0.86
2 ^a	11.2	5.9	5.14 ± 0.02	6.97 ± 0.05
3	4.7	6.6	5.82 ± 0.03	6.77 ± 0.05
4	2.9	9.9	5.76 ± 0.01	6.69 ± 0.04
5	2.0	5.9	5.60 ± 0.03	6.68 ± 0.05
6	1.1	11.1	4.73 ± 0.02	6.70 ± 0.04
7	1.2	14.4	4.51 ± 0.01	6.67 ± 0.03
8	1.9	10.6	4.68 ± 0.01	6.67 ± 0.04
9	1.5	11.4	4.02 ± 0.01	6.68 ± 0.03
10	2.5	7.9	5.07 ± 0.02	6.66 ± 0.04
11	2.9	5.2	7.93 ± 0.06	6.70 ± 0.08
Fuse	2.7	10.5	14.20 ± 0.03	6.67 ± 0.04
Integrated age (2 σ)				198.8 ± 0.8
Plateau age (2 σ)				198.0 ± 0.8
Central High Atlas (intermediate basalt / Telouet) – Sample AN160 – analyzed at Nice (J =0.01720 ; ~ 100 grains)				
Laser steps				
1 ^a	89.6	0.9	17.2 ± 0.3	9.61 ± 2.21
2 ^a	66.0	4.4	38.8 ± 0.4	6.47 ± 0.46
3 ^a	34.7	7.8	53.5 ± 0.4	7.11 ± 0.14
4 ^a	21.3	7.0	57.2 ± 0.7	6.98 ± 0.21
5	21.6	10.8	58.1 ± 0.5	6.87 ± 0.14
6	16.2	11.5	58.4 ± 0.6	6.96 ± 0.13
7	11.0	12.4	58.6 ± 0.4	6.84 ± 0.12
8	9.2	11.8	58.8 ± 0.3	6.91 ± 0.10
9	9.0	13.1	57.4 ± 0.4	6.85 ± 0.11
10 - Fuse	10.2	20.4	58.6 ± 0.1	6.76 ± 0.07
Integrated age (2 σ)				202.0 ± 2.7
Plateau age (2 σ)				201.0 ± 2.4

Table DR4, continuation: $^{40}\text{Ar}/^{39}\text{Ar}$ geochronology of Moroccan CAMP basalts

non radiogenic ^{40}Ar (%)	^{39}Ar (%)	$^{37}\text{Ar}_{\text{Ca}}/^{39}\text{Ar}_{\text{K}}$ $\pm 1\sigma$	$^{40}\text{Ar}_{\text{rad}}/^{39}\text{Ar}_{\text{K}}$ $\pm 1\sigma$	Age (Ma) $\pm 1\sigma$
Central High Atlas (upper basalt/ Oued Lahr) – Sample MOR14, analyzed at Berkeley ($J = 0.001327$; ~20mg)				
Laser Steps (W)				
1.5b	77.9	1.6	72.65 ± 3.20	90.18 ± 5.14
2.5b	85.3	10.4	47.39 ± 0.51	82.92 ± 1.11
3.5b	87.9	12.7	56.68 ± 0.56	86.00 ± 1.55
4.5	55.4	11.6	62.17 ± 0.50	89.27 ± 0.80
5.0	47.4	7.6	63.91 ± 0.70	87.43 ± 1.12
5.5	49.2	7.1	66.06 ± 0.75	89.45 ± 1.20
6.0	53.9	5.3	64.82 ± 0.87	87.30 ± 1.51
6.5	64.1	5.2	66.44 ± 0.97	86.42 ± 1.60
7.5	72.7	5.3	63.58 ± 1.10	86.15 ± 1.91
8.5	75.2	3.8	62.30 ± 1.23	88.86 ± 2.27
9.5	79.3	3.1	58.79 ± 1.31	89.02 ± 3.33
11.0	86.0	4.6	55.97 ± 0.94	87.42 ± 2.02
12.5	82.3	4.3	58.68 ± 1.08	88.50 ± 2.12
14.0	86.7	4.7	60.82 ± 1.11	87.65 ± 2.74
16.0	73.5	4.0	63.66 ± 1.33	87.03 ± 2.37
18.0	71.5	2.8	66.60 ± 1.61	89.08 ± 2.81
21.0	78.9	2.6	71.09 ± 1.91	88.32 ± 3.16
24.0	78.9	1.9	75.76 ± 3.12	89.67 ± 5.91
27.0	78.8	1.6	73.00 ± 3.21	86.74 ± 5.45
				Integrated age (2σ) 198.3 ± 2.3
				Plateau Age (2σ) 199.8 ± 1.8

Table DR5: major and trace element composition of Moroccan CAMP basalts.

sample	AN32	AN37	AN49	AN134	AN136	AN174	AN115b	AN132	AN56	AN18	AN39	AN138
unit	lower	lower	inter	inter	inter	inter						
location	CHA	CHA	CHA	CHA	CHA	Oujda	Argana	Argana	CHA	CHA	CHA	CHA
SiO₂(wt%)	50.88	52.15	53.55	53.57	53.89	53.28	53.14	49.37	53.11	53.23	53.19	53.53
TiO₂	1.21	1.27	1.35	1.43	1.42	1.40	1.37	0.96	1.32	1.22	1.25	1.16
Al₂O₃	11.45	13.53	15.13	14.26	14.09	14.38	14.07	10.02	13.94	14.68	14.49	13.39
FeOt	11.73	10.61	9.09	10.02	10.24	9.65	10.01	12.90	10.66	10.17	10.39	10.31
MnO	0.19	0.15	0.12	0.18	0.17	0.14	0.14	0.21	0.21	0.18	0.17	0.17
MgO	12.86	9.29	6.91	7.23	7.35	7.63	7.24	16.71	7.50	7.34	7.13	8.50
CaO	9.05	10.10	10.53	9.96	9.41	10.17	8.11	7.58	10.48	10.43	10.73	9.94
Na₂O	1.66	1.90	2.13	2.14	2.17	2.17	3.52	1.34	2.06	2.15	2.09	1.90
K₂O	0.71	0.74	0.96	0.98	1.06	0.95	2.23	0.64	0.50	0.41	0.36	0.84
P₂O₅	0.13	0.14	0.15	0.17	0.16	0.17	0.16	0.12	0.15	0.15	0.14	0.17
L.O.I.	0.99	0.67	0.41	0.91	1.34	1.79	2.16	1.74	0.39	0.55	0.35	1.13
Cr (ppm)	236	157	60	92	84	285	303	538	93	72	79	104
Ni	609	502	331	288	267	74	84	377	286	200	233	326
Rb	22.4	23.5	28.3	28.4	20.4	26.7	34.9	22.0	19.4	25.0	36.1	26.83
Sr	176.3	207.5	239.1	237.5	204.5	225.1	302.9	159.8	167.0	172.5	172.5	156.76
Y	20.4	21.0	23.4	26.0	24.3	22.8	23.3	18.7	26.1	24.4	24.3	26.72
Zr	110.7	110.4	126.5	147.2	133.5	131.2	126.4	96.7	117.3	108.7	105.2	129.22
Nb	10.4	10.8	11.9	13.3	12.5	13.0	11.3	8.7	8.8	8.4	8.1	9.95
Cs	1.3	0.7	1.0	0.9	0.8	0.7	0.6	1.8	1.3	1.5	2.1	0.75
Ba	171.3	174.6	202.6	239.7	196.7	214.3	329.5	141.7	156.4	137.3	139.6	188.17
La	12.1	12.5	14.9	15.5	14.9	15.4	13.2	10.6	12.2	11.4	10.9	13.08
Ce	26.4	26.9	31.4	34.3	32.2	33.0	28.7	23.8	26.6	25.0	24.0	29.09
Pr	3.4	3.5	4.0	4.6	4.2	4.3	3.7	3.0	3.5	3.3	3.1	3.75
Nd	14.4	14.4	17.0	18.7	17.8	17.8	15.3	12.6	14.8	13.9	13.4	15.63
Sm	3.5	3.7	4.2	4.6	4.4	4.3	3.9	3.1	3.7	3.5	3.4	3.88
Eu	1.1	1.2	1.3	1.4	1.3	1.4	1.2	0.9	1.2	1.1	1.1	1.15
Gd	3.8	3.9	4.4	4.9	4.6	4.6	4.1	3.3	4.2	3.9	4.1	4.23
Tb	0.6	0.6	0.7	0.8	0.8	0.7	0.7	0.5	0.7	0.6	0.6	0.71
Dy	3.5	3.4	4.1	4.6	4.3	4.3	3.8	3.3	4.2	3.9	4.0	4.34
Ho	0.7	0.7	0.8	0.9	0.9	0.9	0.8	0.6	0.9	0.8	0.8	0.95
Er	2.0	2.0	2.4	2.5	2.6	2.3	2.2	1.8	2.5	2.3	2.4	2.74
Yb	1.9	1.8	1.9	2.3	2.2	2.2	1.9	1.6	2.3	2.2	2.0	2.38
Lu	0.3	0.2	0.3	0.3	0.3	0.3	0.3	0.2	0.3	0.3	0.3	0.35
Hf	2.9	2.8	3.2	3.7	3.5	3.5	3.1	2.4	2.9	2.7	2.7	3.24
Ta	0.6	0.6	0.7	0.8	0.8	0.8	0.7	0.5	0.5	0.5	0.5	0.61
Pb	4.4	3.3	4.2	4.6	4.7	4.5	6.6	4.8	3.9	3.9	3.3	3.66
Th	2.6	2.6	3.0	3.4	3.7	3.7	3.2	2.5	2.5	2.5	2.2	2.87
(La/Yb) cn	4.4	4.6	5.2	4.5	4.5	4.7	4.6	4.4	3.6	3.5	3.6	3.71

Table DR5, continuation: major and trace element composition of Moroccan CAMP basalts.

sample	AN128	AN63	AN22	AN57	AN141	AN164	AN44	AN24	AN156A	AN169
unit	inter	upper	upper	upper	upper	upper	recurrent	recurrent	recurrent	recurrent
location	Argana	CHA	CHA	CHA	CHA	CHA	CHA	CHA	CHA	CHA
SiO₂ (wt%)	52.94	51.60	51.50	51.67	52.05	52.06	50.30	50.58	51.33	51.32
TiO₂	1.26	1.08	1.05	1.09	1.04	1.03	1.61	1.63	1.63	1.56
Al₂O₃	14.38	15.03	15.10	15.05	14.85	15.04	13.69	13.55	13.60	13.59
FeOt	11.43	9.86	9.99	9.86	10.08	9.92	14.88	15.01	14.19	14.36
MnO	0.16	0.16	0.17	0.17	0.18	0.17	0.34	0.28	0.22	0.30
MgO	7.26	8.19	8.00	8.08	7.74	7.99	6.12	5.76	5.93	6.02
CaO	9.94	11.81	11.84	11.73	11.43	11.57	10.45	10.43	10.42	10.29
Na₂O	1.96	1.86	1.92	1.95	1.90	1.83	2.08	2.18	2.13	2.00
K₂O	0.51	0.24	0.27	0.22	0.58	0.23	0.32	0.39	0.34	0.35
P₂O₅	0.15	0.11	0.11	0.11	0.11	0.11	0.17	0.17	0.17	0.16
L.O.I.	1.84	0.51	0.12	0.26	0.58	1.33	0.26	0.65	1.51	0.51
Cr (ppm)	204	89	87	87	91	84	71	72	90	67
Ni	69	205	217	212	229	244	100	105	235	118
Rb	11.00	12.29	11.79	5.51	12.75	14.97	7.52	4.32	6.13	6.30
Sr	248.94	163.96	163.15	172.92	158.81	177.44	92.94	103.86	95.52	102.25
Y	23.06	21.09	20.42	21.32	20.12	20.99	43.10	46.27	41.04	42.99
Zr	109.28	79.04	76.04	80.82	78.05	82.47	115.68	126.09	114.85	123.36
Nb	7.68	5.14	5.03	5.17	4.99	5.25	5.27	5.68	5.21	5.59
Cs	6.68	0.95	0.83	0.72	0.40	0.66	0.50	0.31	0.78	0.59
Ba	109.94	84.27	92.48	102.82	111.89	88.93	178.50	123.26	164.33	120.81
La	10.56	7.48	7.19	7.58	7.17	7.07	8.61	8.90	8.57	8.76
Ce	23.64	16.79	16.45	17.62	16.59	17.23	19.62	20.87	19.85	20.48
Pr	3.07	2.34	2.28	2.36	2.30	2.35	2.72	2.87	2.77	2.78
Nd	13.03	10.23	9.97	10.36	10.35	10.68	13.03	13.22	12.70	13.44
Sm	3.25	2.75	2.70	2.80	2.79	2.88	3.89	4.02	3.92	4.09
Eu	1.05	0.92	0.87	0.94	0.93	0.92	1.24	1.27	1.24	1.28
Gd	3.71	3.20	3.12	3.15	3.14	3.35	5.36	5.60	5.49	5.45
Tb	0.62	0.54	0.54	0.58	0.54	0.58	0.99	1.00	1.00	1.05
Dy	3.69	3.23	3.11	3.26	3.40	3.62	6.41	6.69	6.68	6.87
Ho	0.80	0.73	0.71	0.73	0.72	0.77	1.49	1.53	1.49	1.53
Er	2.26	1.92	1.94	2.06	2.03	2.11	4.44	4.54	4.44	4.63
Yb	2.02	1.83	1.84	2.02	1.87	1.88	3.97	4.52	4.22	4.18
Lu	0.30	0.28	0.29	0.30	0.28	0.29	0.62	0.64	0.64	0.68
Hf	2.72	1.90	2.00	2.04	2.08	2.19	3.05	3.24	3.07	3.26
Ta	0.50	0.30	0.31	0.30	0.31	0.33	0.33	0.35	0.34	0.35
Pb	3.12	1.68	1.73	2.39	2.42	1.73	32.55	4.21	3.32	2.69
Th	2.35	1.19	1.23	1.28	1.27	1.36	2.08	2.31	2.14	2.16
(La/Yb) cn	3.52	2.75	2.64	2.52	2.58	2.53	1.46	1.33	1.37	1.41

Table DR6: magnetostratigraphy of Central High Atlas section.

Formation	Flow	n	V_{Long}	V_{Lat}	D_p	D_m	A₉₅	Paleolat
upper	34	8	271.2	63.4	4.9	7.9	6.4	24.9
upper	33	7	281.7	66.6	5.6	8.4	6.4	30.0
intermediate	32	3	280.4	60.9	5.6	8.7	6.7	28.2
intermediate	31	4	279.2	63.0	4.8	7.4	5.8	28.2
intermediate	30	6	282.8	62.0	2.7	4.2	2.8	29.5
intermediate	29	5	284.5	65.4	3.7	5.5	4.1	30.9
intermediate	28	6	277.3	64.6	5.7	8.9	6.1	27.8
sediments	(27)	3	109.4	-37.3	6.0	12	4.1	-30.3
intermediate	26	5	251.5	67.6	4.9	8.5	7.4	19.6
intermediate	25	4	265.6	61.7	5.7	9.7	6.8	20.9
intermediate	24	4	264.4	62.5	3.7	6.2	5.2	21.7
intermediate	23	4	258.4	66.0	3.2	5.4	4.6	21.0
lower	22	5	120.7	76.0	2.2	3.5	4.2	25.7
lower	21	5	113.7	75.1	1.0	1.5	5.4	28.4
lower	20	3	121.8	79.3	5.5	8.8	7.0	26.2
lower	19	4	115.0	79.5	4.4	6.9	5.4	27.4
lower	18	6	120.2	80.1	2.1	3.2	2.8	27.2
lower	17	4	143.7	84.9	3.7	5.8	4.5	27.3
lower	16	3	109.0	82.9	7.9	12.1	9.2	29.4
lower	15	3	178.2	87.3	6.9	10.8	8.5	27.4
lower	14	4	137.5	82.7	2.2	3.5	2.8	26.2
lower	13	4	129.0	83.8	4.5	7.0	2.6	27.5
lower	12	4	129.3	81.0	4.2	6.7	6.3	26.5
lower	11	4	141.3	82.7	2.9	4.6	4.5	26.1
lower	10	4	115.0	78.6	3.8	6.0	4.7	27.1
lower	9	6	133.3	82.2	3.4	5.4	5.0	25.7
lower	8	6	203.3	79.8	3.2	5.4	4.5	21.3
lower	7	5	213.9	78.6	2.5	4.3	4.8	21.8
lower	6	4	212.4	78.5	2.1	3.5	3.6	20.2
lower	5	3	182.3	77.1	2.9	5.1	4.5	18.3
lower	4	4	183.8	77.1	2.9	5.1	4.5	18.2
lower	3	4	205.2	77.1	2.8	4.9	4.3	18.7
lower	2	3	192.3	77.5	3.0	5.2	5.0	19.4
lower	1	6	205.9	76.8	2.7	4.8	4.3	18.6

NOTE: Tilt correction applied to the Tiourjdal flows is 12° - 15° dip, with 200° - 205° dip direction.